NASA TECHNICAL MEMORANDUM

NASA TM X-1634

NASA TM X-1634

STUDY OF OPTICAL RADIATION IN THE WAVELENGTH REGIONS OF 0.4216μ, 0.4278μ, 0.4835μ, AND 0.5165μ BEHIND NORMAL SHOCK WAVES IN A SIMULATED MARTIAN ATMOSPHERE

by

Anthony P. Modica and Harry B. Dyner
Avco Corporation

and

Henry T. Woodward and James O. Arnold
Ames Research Center

NATIONAL AERONAUTICS AND SPACE ADMINISTRATION • WASHINGTON, D. C. • AUGUST 1968

NASA TM X-1634

STUDY OF OPTICAL RADIATION IN THE WAVELENGTH REGIONS OF 0.4216μ, 0.4278μ, 0.4835μ, AND 0.5165μ BEHIND NORMAL SHOCK WAVES IN A SIMULATED MARTIAN ATMOSPHERE

By Anthony P. Modica and Harry B. Dyner

Avco Corporation
Wilmington, Mass.

and

Henry T. Woodward and James O. Arnold

Ames Research Center
Moffett Field, Calif.

NATIONAL AERONAUTICS AND SPACE ADMINISTRATION

For sale by the Clearinghouse for Federal Scientific and Technical Information
Springfield, Virginia 22151 – CFSTI price $3.00

STUDY OF OPTICAL RADIATION IN THE WAVELENGTH REGIONS
OF 0.4216μ, 0.4278μ, 0.4835μ, AND 0.5165μ
BEHIND NORMAL SHOCK WAVES IN A
SIMULATED MARTIAN
ATMOSPHERE

By Anthony P. Modica and Harry B. Dyner

Avco Corporation

and

Henry T. Woodward and James O. Arnold

Ames Research Center

SUMMARY

Shock-tube measurements of equilibrium and nonequilibrium radiation in a 50-percent CO_2 - 50-percent N_2 gas mixture are analyzed and compared to theoretical estimates and other measurements. The ratio of the integrated radiation from the nonequilibrium zone behind the normal shock wave to the equilibrium radiation from an equal volume of gas is of particular interest. The measurements show no appreciable differences in nonequilibrium enhancement from four different spectral regions.

INTRODUCTION

Characteristics of optical radiation from shock-tube experiments simulating Mars entry are analyzed and compared to those from theory and other measurements. The results will be useful in studies directed toward determining the composition of the Mars atmosphere from shock-layer radiation measurements taken on board a probe vehicle during entry.

Measurements in a 50-percent CO_2 - 50-percent N_2 gas mixture were obtained at velocities from 5 to 7 km/sec and initial shock-tube-loading pressures from 2000 to 50 μ Hg. Narrow-band filtered radiometers were used to isolate for study the spectral regions around 0.4216μ, 0.4278μ, 0.4835μ, and 0.5165μ. The shock-tube measurements were conducted, under contract, in the Experimental Gas Dynamic Section of the Aerophysics Laboratory, at the Avco Space Systems Division's Research and Technology Laboratories, and the data were analyzed at Ames Research Center.

SYMBOLS

I	radiative intensity, W/cm^3-μ-sr
I_p	peak radiative intensity, W/cm^3-μ-sr
I_e	equilibrium radiative intensity, W/cm^3-μ-sr
I_{th}	theoretical spectral intensity, W/cm^3-μ-sr
K	radiometer calibration constant, W/cm^3-μ-sr-mV
p_1	gas pressure ahead of shock wave, μ Hg
p_o	standard earth atmospheric pressure, 7.6×10^5 μ Hg
R_λ	radiometer filter transmission normalized to unity, dimensionless
t	laboratory time measured from shock front, μsec
U_s	shock velocity, km/sec
λ	wavelength, μ
$\tau_{1.1}$	laboratory time elapsed until radiation decays to 110 percent of equilibrium level, μsec
σ	amount of nonequilibrium radiative enhancement for normal shocks, $\int^{\tau_{1.1}} I(t)dt/I_e\tau_{1.1}$, dimensionless

EXPERIMENTAL FACILITY AND PROCEDURE

The facility used for the study was a combustion-driven shock tube (fig. 1). It consists of a 15-foot driven section made of 6-inch inside diameter Pyrex pipe and stainless-steel tubing. The tubing is coupled by a 2-foot-long conical transition section to a 2.5-foot-long driver section of 1.5-inch inside diameter. The test section was mounted 12 feet from the end of the transition section between the two lengths of Pyrex pipe.

To determine shock speeds, shock-front emission was measured by collimated (1 mm diam.) photomultipliers at four stations upstream and two downstream of the test section. The outputs of the photomultipliers were doubly differentiated and displayed on a time-mark folded Tektronix 535A oscilloscope (sweep-driven by a Radionic's (model TWN-2A) triangular wave and marker timing generator). Shock transit times measured with this instrument are accurate to ±1 percent.

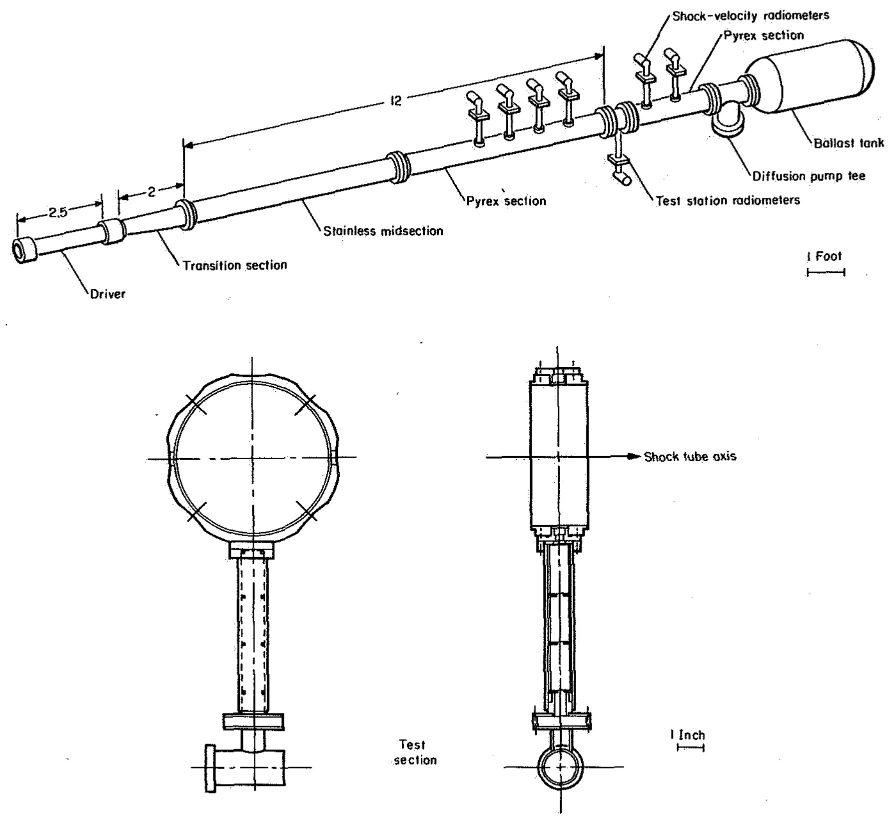

Figure 1.- Diagram of experimental apparatus and optical system.

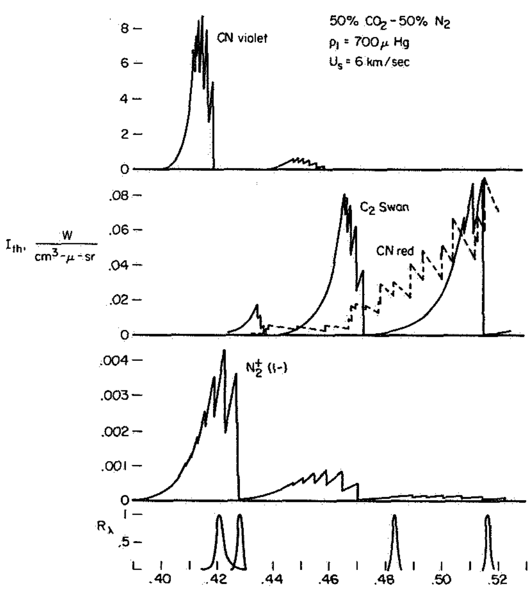

Figure 2.- Spectral intensities and filter transmission values.

Four spectral regions were selected to isolate prominent features in the molecular band spectra characteristic of gas mixtures containing CO_2 and N_2. Figure 2 shows the spectral intensities of band systems obtained from reference 1 for a shock velocity of 6 km/sec and an initial pressure of 700 μ Hg. The radiometer band passes were centered at 0.4216μ, 0.4278μ, 0.4835μ, and 0.5165μ to measure radiation from bands of CN violet, N_2^+ (1-) plus C_2 Swan, CN red, and C_2 Swan plus CN red, respectively.

Each of the four radiometers (one of which is detailed in fig. 1) consists of a collimating slit 0.5 mm by 12.7 mm alined with the long dimension parallel to the shock wave, a narrow-band interference filter, and either an RCA 1P21 or 1P28 photomultiplier tube, the output of which is coupled to a cathode follower.

The relative transmission of each filter is shown in figure 2. The finite width viewing slit was the dominant factor in the radiometer rise time. With the slit arrangement used, the optical rise time for an incident shock velocity around 6 km/sec was, at most, 300 μsec.

The four radiometers were positioned radially at the test section (fig. 1), and the output of each was recorded on both channels of a Tektronix 555 dual-beam oscilloscope. Tektronix type K, CA, and B preamplifier units (less than 50 μsec rise time) were used. One channel of the oscilloscope was used to obtain equilibrium radiation intensities, while the other was delayed internally and swept at a faster rate so as to show the nonequilibrium overshoot radiation profiles better.

For the photometric calibration of the entire optical system (including the quartz shock-tube window, optical interference filter, and photodetector) a tungsten filament lamp was used as an extended source. The lamp was calibrated with an optical pyrometer and with the spectral characteristics of tungsten given by DeVos (ref. 2). During calibration of the optical system, the lamp and radiometers were positioned to simulate the geometry of the shock-tube setup. The windows were cleaned each day before calibration. Both the windows and the shock tube were cleaned after every fifth shock-tube run. A correction for transmission losses between calibrations (due to contaminant on the window) was necessary. The transmittance of the window was estimated to decrease by approximately 5 percent per run.

The gas mixture prepared for study in this investigation consisted of 50-percent CO_2 and 50-percent N_2 partial pressures. Matheson research grade N_2 and CO_2 (99.996-percent purity) were used. Mass spectrometric analysis of the gas mixture showed the specified composition to be accurate to 0.1 percent.

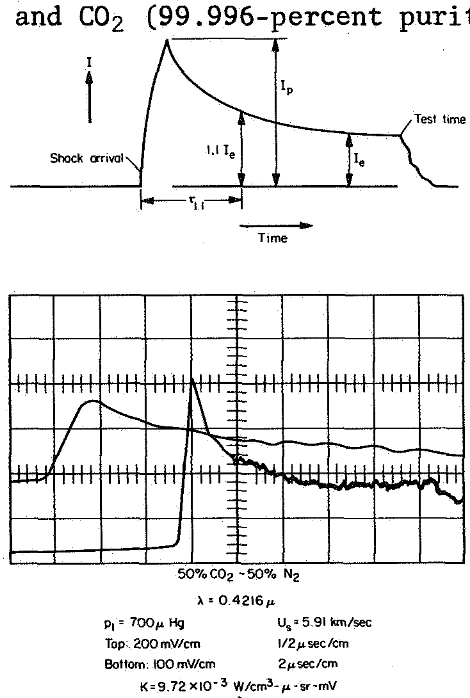

Figure 3.- Oscillogram record of test gas radiation behind incident shock wave.

In general, the experimental procedure involved evacuating the shock tube to less than 1 μ Hg with a 4-inch oil diffusion pump located between the driven section and dump tank (the leak rate of the driven section and gas-handling system was less than 1 μ Hg per min). The test gas was introduce until a pressure of at least 15 mm Hg was reached and was allowed to equilibrate to ambient temperature in about 3 minutes. The shock tube was then evacuated to the desired initial pressure. Since all runs were conducted at initial pressures between 50 and 2000 μ Hg, this procedure helped eliminate any residual air from the tube. Combustion driving with H_2-O_2 and H_2-O_2-He mixtures against 5,000 to 10,000 psia scribed steel diaphragms was used to obtain shock velocities from 5 to 7 km/sec. The radiation profiles monitored behind incident shock waves into ambient pressures from 50 to 2000 μ Hg invariably exhibited radiation overshoots at the front with a subsequent decay in intensity as can be seen from the example oscillogram in figure 3.

ANALYSIS OF MEASUREMENTS

The measurements of normal shock properties described above have been obtained for conditions of velocity and ambient pressure corresponding to typical Mars entry trajectories. Discussed are time to reach equilibrium, equilibrium intensities, and the total integrated radiation from the nonequilibrium zone.

Because of the expected low atmospheric pressures on Mars, the total integrated radiation from the nonequilibrium zone is of particular interest. Equilibrium intensities are also of interest, but to a lesser degree than the nonequilibrium properties. To establish these quantities the extent of the nonequilibrium zone must be determined. It has been defined herein, in conformity with recent practice in this subject, as the zone of gas in the radiation overshoot region which extends behind the shock until the radiation is within 10 percent of the equilibrium level. Many of the oscillograms from the present measurements, however, fail to exhibit clearly an "apparent" equilibrium level, making it difficult to determine the position along the trace where the nonequilibrium zone terminates. An alternative procedure is to use known values of the extent of the nonequilibrium zone. Predicted values of the time to reach 1.1 of the equilibrium level obtained from the analytical model of reference 3 are shown by the curves in figure 4. Selected measurements of $\tau_{1.1}$ from all four spectral regions having more clearly defined "apparent" equilibrium levels are listed in table I and plotted in figure 4. Evidence of the validity of the predicted $\tau_{1.1}$ values is shown by the agreement with the measured values. Because of their consistency and apparent validity, the predicted $\tau_{1.1}$ values were used to obtain the equilibrium intensities and nonequilibrium properties.

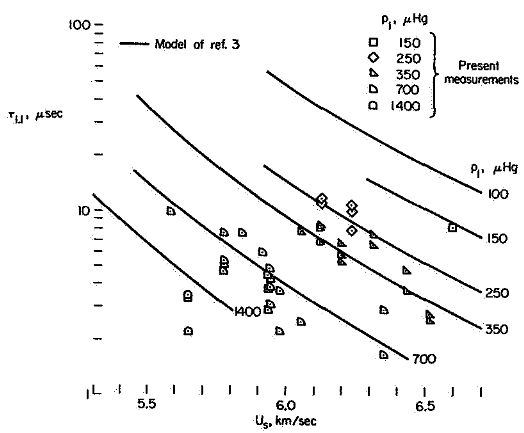

Figure 4.- Measurements of the time for radiative decay to 110% of equilibrium intensity; 50% CO_2-50% N_2.

The measured equilibrium intensities are listed in table I. They can be compared with the predicted spectral intensities of reference 1 by summing the contributions of band systems in the filter spectral range and accounting for filter transmission. Thus, the theoretical equilibrium intensity is

$$I_e = \frac{\int_{\lambda_1}^{\lambda_2} I_{th} R_\lambda \, d\lambda}{\int_{\lambda_1}^{\lambda_2} R_\lambda \, d\lambda}$$

where I_{th} is the spectral intensity of the contributing systems and R_λ is the filter transmission function. The integration is performed over all nonzero values of the integrand.

The measurements were made at various shock-tube pressures. Since comparison of theory and experiment is more convenient if the pressure effects are deleted, the pressure dependence of the theoretical value of I_e was determined by fitting expressions of the form $I_e = k(p_1/p_0)^n$ over the velocity range and evaluating n. Both predicted and measured values of I_e were then normalized by $(p_1/p_0)^n$. The value of n was determined to give the best fit at a velocity intermediate in the test velocity range, and it is this value which is used in figure 5. The spreading of the theory curves at the extreme velocities is a consequence of the variation of n with velocity.

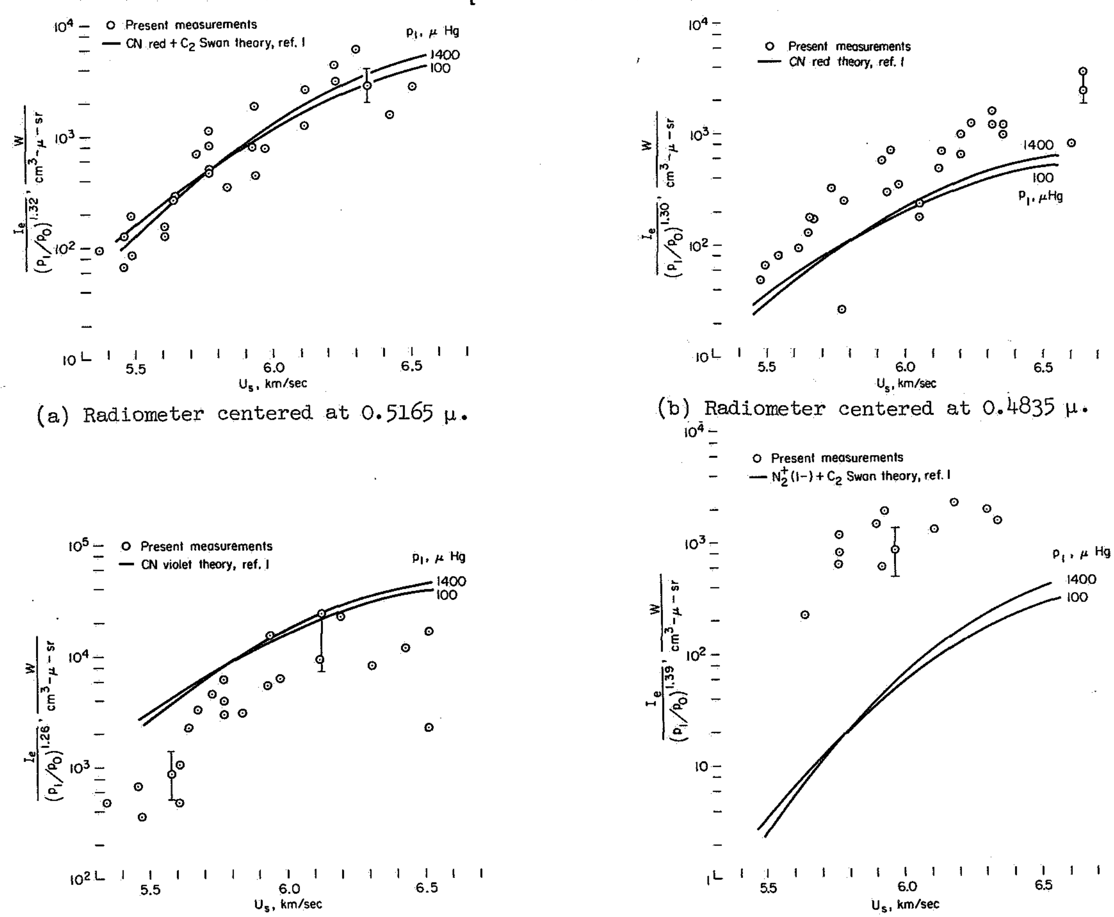

(a) Radiometer centered at 0.5165 μ.

(b) Radiometer centered at 0.4835 μ.

(c) Radiometer centered at 0.4216 μ.

(d) Radiometer centered at 0.4278 μ.

Figure 5.- Comparison of equilibrium predictions and measurements in 50% CO_2-50% N_2.

The good agreement between the present measurements and the predictions in the 0.5165μ region shown in figure 5(a) is support for the CN Red and C_2 Swan predictions of reference 1. The C_2 Swan predictions are also supported by the measurements of reference 4 and with some new (as yet unpublished) measurements at Ames Research Center. With respect to velocity dependence there is fair agreement between measurements and predictions in the 0.4835μ and 0.4216μ regions (figs. 5(b) and 5(c)). The predictions of absolute intensity in the 0.4216μ region are in essential agreement with three independent measurements (refs. 3, 5, and 6) and are considered reasonably well determined. In view of this and the good agreement in the 0.5165μ region, inconsistencies in the absolute intensities of the present measurements are suggested by the overprediction of one CN band system in the 0.4216μ region and the underprediction of another CN band system in the 0.4835μ region. In addition, the prediction for the 0.4278μ region, shown in figure 5(d), is too low by ten times.

In the two radiometer channels which are underpredicted (figs. 5(b) and 5(d)) the excess equilibrium radiation is not believed to be the result of shock-tube impurities, since the four radiometers did not indicate any detectable radiation in experiments conducted in nitrogen-argon mixtures under similar temperature and density conditions. The fact that the general level of the expected radiation is lower than it is for the other two radiometers suggests that possibly the difficulty is due to radiation being observed outside the band pass of the spectral filter. This possibility could only be discounted by measurements of the filter transmission over wide spectral ranges, and these have not been performed.

Nonequilibrium Integrated Intensity

The fundamental radiative property of interest here is the total integrated emission from the nonequilibrium zone. This property is most easily described by comparing it to the equilibrium emission from an equal volume of gas. Such a comparison also eliminates the effect of possible absolute calibration errors. This comparison can be expressed as a ratio, given by the parameter

$$\sigma = \frac{\int_0^{\tau_{1.1}} I(t)dt}{I_e \tau_{1.1}}$$

Values of σ obtained from the measured values of $I(t)$ and I_e, and the predicted values of $\tau_{1.1}$ are listed in table I and plotted in figure 6. It should be noted that these values of σ are for one-dimensional flow and are expected to be somewhat modified when applied to flow in vehicle shock layers. Interestingly, a comparison of values in the four spectral regions shows that they are not appreciably different. In the 0.4216μ region, in particular, the agreement between the present measurements and those of reference 3 is excellent. The theoretical model of reference 3, which is

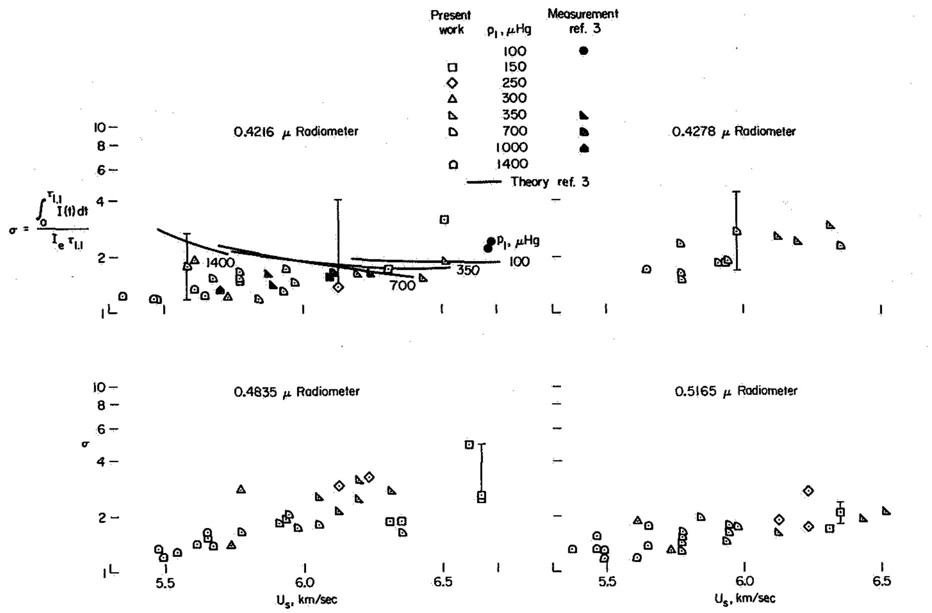

Figure 6.- Values of integrated radiation observed in nonequilibrium zone compared with equilibrium emission from an equal volume of gas; 50% CO_2-50% N_2.

based upon data collected above about 5.8 km/sec, agrees well with the magnitude of the measurements obtained at the higher velocities but not with the slope. Since the product of I_e and $\tau_{1.1}$ is almost independent of pressure and since binary scaling makes $\int_0^{\tau_{1.1}} I(t)dt$ independent of pressure, it follows that the theoretical value of σ should show only a weak pressure dependence, as can be seen in figure 6.

At lower velocities, the theoretical model overpredicts both the present measurements and those of reference 3. Evidence that the model may be invalid in this regime is given in reference 3, where it is shown that the model predicts peak intensities about twice those measured at 5.5 km/sec for a 25-percent CO_2 - 75-percent N_2 mixture.

CONCLUSIONS

In conclusion, it is felt that the present work exhibits two important features. The first is that the nonequilibrium radiative enhancement (given by the parameter σ) is not large for normal-shock flows in a 50-percent CO_2 - 50-percent N_2 gas mixture. Secondly, it is most interesting to note that the nonequilibrium enhancement is quite similar for all four spectral regions studied in the experiment.

Ames Research Center
National Aeronautics and Space Administration
Moffett Field, Calif., 94035, May 7, 1968
124-07-01-07-00-21

REFERENCES

1. Woodward, Henry T.: Predictions of Shock-Layer Radiation From Molecular Band Systems in Proposed Planetary Atmospheres. NASA TN D-3850, 1967.

2. DeVos, J. C.: A New Determination of the Emissivity of Tungsten Ribbon. Physica, vol. 20, no. 10, Oct. 1954, pp. 690-714.

3. McKenzie, Robert L.; and Arnold, James O.: Experimental and Theoretical Investigations of the Chemical Kinetics and Nonequilibrium CN Radiation Behind Shock Waves in CO_2-N_2 Mixtures. AIAA Paper 67-322.

4. Fairbairn, A. R.: A Shock Tube Study of the Oscillator Strength of the C_2 Swan Bands. Res. Rep. 227, Avco-Everett, Aug. 1965.

5. Reis, Victor H.: Oscillator Strength of the CN Violet System. J. Quant. Spectrosc. Radiat. Transfer, vol. 5, no. 4, July/August 1965, pp. 585-594.

6. Whiting, Ellis E.: Determination of Mars Atmospheric Composition by Shock-Layer Radiometry During a Probe Experiment. AIAA Paper 67-293.

TABLE I.- 50 PERCENT CO_2 - 50 PERCENT N_2 MIXTURE

p_1, μ Hg	U_s, km/sec	I_e, watts/cm^3-μ-sr				σ				$\tau_{1.1}$, μsec			
		0.4216μ	0.4278μ	0.4835μ	0.5165μ	0.4216μ	0.4278μ	0.4835μ	0.5165μ	0.4216μ	0.4278μ	0.4835μ	0.5165μ
150	6.35			1.973 -2	3.49 -2			1.9	2.1				
	6.64			3.985 -2				2.57					
	6.597			1.347 -2				4.915				8.2	
	6.31	1.773 -1		2.61 -2	7.48 -2	1.773		1.9	1.713				
	6.64			5.92 -2				2.6					
	6.513	4.825 -2				3.218							
250	6.235				7.55 -2				1.761				10.8
	6.125	9.71 -1		2.17 -2	6.44 -2	1.4		2.948	1.924			11.75	11.1
	6.235			3.93 -2	1.05 -1			3.27	2.768			7.8	10.1
	5.73	2.35 -1		1.263 -2	2.22 -2	1.23		1.398	1.301				
	5.77			1.035 -3				2.8					
	5.61	2.495 -2			4.09 -3	1.96			1.885				
350	6.195			4.82 -2				2.476				5.7	
	6.12	5.85 -1	2.89 -2	2.35 -2	4.76 -2	1.6	2.64	2.123	1.627	8.3	8.15	6.8	
	6.195	1.413	4.99 -2	3.2 -2		1.639	2.488	3.115			5.24	6.65	
	6.513	1.025			1.055 -1	1.915			2.109	2.72			2.53
	6.311		4.33 -2	5.94 -2			3.03	2.754			7.48	6.55	
	6.43	7.42 -1			5.96 -2	1.549			1.92	4.78			3.68
	6.048			8.68 -3				2.55				7.7	
700	5.582	1.33 -1				1.8				9.8			
	5.773				1.09 -1				1.558				4.7
	5.94	2.315	1.126 -1	8.42 -2	1.825 -1	1.735	1.985	2.07	1.788		3.08	4.85	3.83
	5.77	3.74 -2	3.74 -2		7.89 -2	1.686	2.428		1.3				
	5.773		6.96 -2				1.545						
	5.773	5.84 -1	4.82 -2		4.87 -2	1.52	1.675		1.452	5.18			5.3
	5.677	4.9 -1				1.55							
	5.976	9.46 -1	5.015 -2	4.125 -2	7.52 -2	1.48	2.8	1.755	1.741			2.2	3.65
	5.907		8.59 -2	6.74 -2			1.9	1.844				5.94	
	5.93	8.09 -1	3.52 -2	3.52 -2	7.67 -2	1.326	1.915	1.922	1.47	4.42		3.72	2.85
	6.35		8.81 -2	1.17 -1			2.358	1.629			1.66	2.9	
	5.942				4.26 -2				1.631				4.23
	5.839	4.85 -1			3.34 -2	1.21			1.983				7.55
	5.773	4.53 -1		2.92 -2	4.52 -2	1.484		1.662	1.652	7.45			
	6.048			2.8 -2				1.811				2.5	
1400	5.462	1.73 -1				1.232							
	5.462	2.44 -1			1.634 -2	1.2			1.575				
	5.664			4.92 -2				1.395					
	5.376				2.31 -2				1.33				
	5.462				3.105 -2				1.325				
	5.492			1.769 -2	2.08 -2			1.23	1.18				
	5.61	3.82 -1		2.71 -2	3.76 -2	1.364		1.43	1.185				
	5.475	1.3 -1		1.405 -2		1.199		1.365					
	5.645	8.19 -1	3.54 -2	3.76 -2	6.62 -2	1.245	1.737	1.66	1.375	2.2		3.4	3.47
	5.49				4.62 -2				1.3				
	5.65			5.17 -2	7.1 -2			1.546	1.766				
	5.54			2.34 -2				1.304					

Note: A group of digits followed by -n indicates that the decimal [illegible] the first digit.

NASA-Langley, 1968 —— 12 A-2887

"The aeronautical and space activities of the United States shall be conducted so as to contribute . . . to the expansion of human knowledge of phenomena in the atmosphere and space. The Administration shall provide for the widest practicable and appropriate dissemination of information concerning its activities and the results thereof."

—National Aeronautics and Space Act of 1958

NASA SCIENTIFIC AND TECHNICAL PUBLICATIONS

TECHNICAL REPORTS: Scientific and technical information considered important, complete, and a lasting contribution to existing knowledge.

TECHNICAL NOTES: Information less broad in scope but nevertheless of importance as a contribution to existing knowledge.

TECHNICAL MEMORANDUMS: Information receiving limited distribution because of preliminary data, security classification, or other reasons.

CONTRACTOR REPORTS: Scientific and technical information generated under a NASA contract or grant and considered an important contribution to existing knowledge.

TECHNICAL TRANSLATIONS: Information published in a foreign language considered to merit NASA distribution in English.

SPECIAL PUBLICATIONS: Information derived from or of value to NASA activities. Publications include conference proceedings, monographs, data compilations, handbooks, sourcebooks, and special bibliographies.

TECHNOLOGY UTILIZATION PUBLICATIONS: Information on technology used by NASA that may be of particular interest in commercial and other non-aerospace applications. Publications include Tech Briefs, Technology Utilization Reports and Notes, and Technology Surveys.

Details on the availability of these publications may be obtained from:

SCIENTIFIC AND TECHNICAL INFORMATION DIVISION

NATIONAL AERONAUTICS AND SPACE ADMINISTRATION

Washington, D.C. 20546